Lehtonen, Janika; Chen, Xiao; Beaumont, Marco; Hassinen, Jukka; Orelma, Hannes; Dumée, Ludovic F.; Tardy, Blaise; Rojas Gaona, Orlando

Impact of incubation conditions and post-treatment on the properties of bacterial cellulose membranes for pressure-driven filtration

Published in:
Carbohydrate Polymers

DOI:
10.1016/j.carbpol.2020.117073

Published: 01/01/2021

Document Version
Peer-reviewed accepted author manuscript, also known as Final accepted manuscript or Post-print

Journal Pre-proof

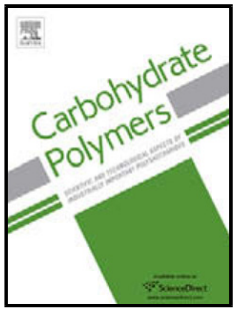

Impact of incubation conditions and post-treatment on the properties of bacterial cellulose membranes for pressure-driven filtration

Janika Lehtonen (Conceptualization) (Methodology) (Investigation) (Writing - original draft) (Visualization), Xiao Chen (Investigation) (Writing - review and editing), Marco Beaumont (Investigation) (Writing - review and editing), Jukka Hassinen (Conceptualization) (Writing - review and editing), Hannes Orelma (Conceptualization) (Writing - review and editing), Ludovic F. Dumée (Conceptualization) (Writing - review and editing) (Supervision), Blaise L. Tardy (Conceptualization) (Writing - original draft) (Supervision), Orlando J. Rojas (Conceptualization) (Writing - review and editing) (Supervision)<ce:contributor-role>Funding aquisition)

PII: S0144-8617(20)31246-7

DOI: https://doi.org/10.1016/j.carbpol.2020.117073

Reference: CARP 117073

To appear in: *Carbohydrate Polymers*

Received Date: 25 June 2020

Revised Date: 13 August 2020

Accepted Date: 5 September 2020

Please cite this article as: Lehtonen J, Chen X, Beaumont M, Hassinen J, Orelma H, Dumée LF, Tardy BL, Rojas OJ, Impact of incubation conditions and post-treatment on the properties of bacterial cellulose membranes for pressure-driven filtration, *Carbohydrate Polymers* (2020), doi: https://doi.org/10.1016/j.carbpol.2020.117073

Impact of incubation conditions and post-treatment on the properties of bacterial cellulose membranes for pressure-driven filtration

Janika Lehtonen[a], Xiao Chen[b], Marco Beaumont[a], Jukka Hassinen[a], Hannes Orelma[c], Ludovic F. Dumée[b,d]*, Blaise L. Tardy[a]*, Orlando J. Rojas[a,e]*

[a] Department of Bioproducts and Biosystems, School of Chemical Engineering, Aalto University, P. O. Box 16300, FI-00076 Aalto, Espoo, Finland

[b] Deakin University, Geelong, Institute for Frontier Materials, Waurn Ponds, Victoria 3216, Australia

[c] VTT - Technical Research Centre of Finland, Tietotie 4E, P.O. Box 1000, FI-02044 Espoo, Finland

[d] Department of Chemical Engineering, Khalifa University of Science and Technology, P.O. Box 127788, Abu Dhabi, United Arab Emirates

[e] Departments of Chemical & Biological Engineering, Chemistry, and Wood Science, The University of British Columbia, Vancouver, British Columbia V6T 1Z3, Canada

*Corresponding authors: Blaise L. Tardy (blaise.tardy@aalto.fi, phone: +358 505979156), Ludovic F. Dumée (ludovic.dumee@deakin.edu.au, phone: +61-410131312) and Orlando J. Rojas (orlando.rojas@ubc.ca, phone: +1-6048223457)

Graphical abstract

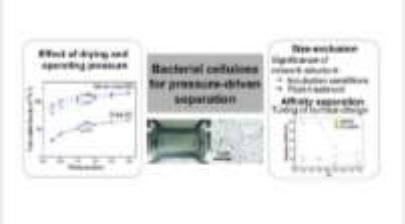

Abstract

Bacterial cellulose (BC) has shown potential as a separation material. Herein, the performance of BC in pressure-driven separation is investigated as a function of incubation conditions and post-culture treatment. The pure water flux of never-dried BC (NDBC), was found to be 9 to 16 times higher than that for dried BC (DBC), in a pressure range of 0.25 to 2.5 bar. The difference in pressure response of NDBC and DBC was observed both in cross-flow filtration and capillary flow porometry experiments. DBC and NDBC were permeable to polymers with a hydrodynamic radius of ~60 nm while protein retention was possible by introducing anionic surface charges on BC. The results of this work are expected to expand the development of BC-based filtration membranes, for instance towards the processing of biological fluids.

Keywords: bacterial cellulose, nanocellulose, filter, pure water flux, separation, compression

1 Introduction

Membranes produced from bacterial cellulose (BC), are highly appealing in material development. BC is produced at the air-water interface by aerobic bacteria, producing nanofibers with diameters in the range of 20 to 100 nm (Klemm et al., 2011). In addition to its sustainable production, BC possesses several outstanding properties, including high mechanical strength (Nishi et al., 1990; Iguchi et al., 2000), high temperature tolerance (George et al., 2008), high

resistance to dissolution in most solvents (Liebert, 2010), and contains abundant surface hydroxyl groups that facilitate chemical modification. Furthermore, high purity cellulose I isolated from BC does not trigger significant inflammatory response and has good compatibility with living tissues (Fu et al., 2013). This combination of properties has resulted in various applications in the biomedical field. BC has been used as barrier material, where control over permeation of biological fluids and their macromolecules is quintessential (Gonçalves et al., 2015). In wound healing, the permeation properties of the BC network allow air access to the wound while preventing the passage of bacteria and other pathogens. In addition to biomedical applications, the unique 3D network structure of BC has been utilized to obtain robust porous materials such as carbon structures (Wu et al., 2013), networks containing several types of functional particles (Roig-Sanchez et al., 2019), and membranes for pervaporation (Dubey et al., 2002; Pandey et al., 2005), membrane distillation (Camacho et al., 2013; Leitch et al., 2016), and electroacoustic transduction (Nishi et al., 1990).

3D networks of entangled nanofibers, such as those present in BC, have unique behavior compared to networks of conventional polymeric or isotropic particles. For instance, compression of fibers oriented in a pseudo-nematic or chiral-nematic order results in pore size harmonization, with a preferential reduction of pore sizes in the lateral dimensions (Plappert et al., 2017; Tripathi et al., 2019). As most cellulosic hydrogels, those from BC do not recover upon compression, which is ascribed to cellulose-cellulose supramolecular interactions induced by fiber-fiber contacts. The network architecture and properties of BC can be controlled by varying the culture conditions. For instance, the fibril size, surface area, and porosity of BC depend on the activity of the producing organism, composition of the culture medium and the carbon source used (Ul-islam et al., 2012).

In most applications involving separation, variables such as pressure, chemical gradients, and surface adsorption affect filtration performance in terms of flux and selectivity. Due to the excellent water retaining capacity in the never-dried state (generally a hydrogel containing 99% water) (Gelin et al., 2007), the characteristics of the BC network depend on the presence of defects, membrane compression and other parameters affecting the surface of the fibers. Thus, the flux and the separation potential of BC depend on (i) the cultivation conditions, (ii) post-culture treatment and pre-compression/dewatering of the network, and (iii) the processing variables during separation such as pressure applied to the system (Abedini et al., 2011; Carreño Pineda et al., 2010; Takai et al., 1991).

The performance of never-dried BC (NDBC) and BC composites have been evaluated for specific membrane-associated applications such as oil-water (Galdino et al., 2020; Hassan et al., 2017) and catalytic (Xu et al., 2018) membrane separation as well as size-exclusion filtration (Jiang et al., 2019). Towards the latter endeavor, BC filtration and permeation characteristics have been considered (Carreño Pineda et al., 2010; Shibazaki et al., 1993; Sokolnicki et al., 2006; Takai et al., 1991). Mechanically-treated or disintegrated BC has also been examined in separation systems as self-standing nanopapers (Mautner et al., 2015) or by incorporation in other types of networks (Tabuchi & Baba, 2005; Tang et al., 2019). However, it should be noted that disintegration of BC destroys the inherent structuring of its pellicles and demands energy. Although the material properties of BC have been widely studied (Iguchi et al., 2000), the factors affecting properties relevant for pressure-driven separation, such as pure water fluxes (PWFs) and separation potential, have not been evaluated comprehensively, particularly, in efforts to compare NDBC and the dried counterpart, DBC. This work presents, for the first time, a comprehensive

investigation on the effects of variables (i-iii, as introduced earlier) on the filtration properties of BC.

Since pressure was expected to have a significant role on the permeation properties of BC, cross-flow filtration experiments and capillary flow porometry were used to elucidate how the NDBC and DBC membranes respond to pressure. Next, DBC membranes obtained under different incubation conditions (incubation time and addition of poly(oxyethylene) (POE) to culture medium) and *ex situ* modification (acetone treatment post-incubation) were used to assess the impact on permeation properties and membrane surface morphology. Lastly, the effect of surface charge on separation of bovine serum albumin (BSA) is studied by comparing unmodified and TEMPO-oxidized (negatively charged) BC. The results of this study provide insights towards the variable ways to control flux and separation across BC membranes, giving novel information on the possibilities and challenges for implementing BC for pressure-driven separation. Further developments in applications utilizing the hydrophilicity of BC, for solvent dehydration or oil-water separation or, more importantly, novel directions in the biomedical field, are expected to benefit from the insights provided in this study.

2 Materials and Methods

2.1 Materials

Komagataeibacter medellinensis (previously named *Gluconacetobacter medellinensis*) (Castro et al., 2013) was used as the strain to produce BC and was provided by the School of Engineering, Universidad Pontificia Bolivariana, Colombia. D-(+) –Glucose was obtained from VWR and Sigma Aldrich. Yeast extract, peptone, sodium phosphate dibasic, citric acid, 2,2,6,6-Tetramethylpiperidine 1-oxyl (TEMPO), BSA (molecular weight 66 kDa), and POE (average molecular weights 0.01, 0.1, 0.4 1 and 2 MDa) were obtained from Sigma-Aldrich. Sodium bromide was obtained from Riedel-de Haën and sodium hypochlorite from VWR. All chemicals were used as received.

2.2 Synthesis and modification of bacterial cellulose membranes

BC was synthesized using the modified Hestrin-Schramm (HS) medium consisting of 20 g/L glucose, 5 g/L yeast extract, 5 g/L peptone and 2.5 g/L sodium phosphate dibasic and the pH was adjusted to 4.5 with citric acid. The medium was sterilized by boiling for 15 min and *K. medellinensis* was statically incubated at 28 °C in plastic containers (20 cm x 30 cm) with 2.5 L culture medium. The culture medium was inoculated with 50 mL of preculture grown for two days to produce the BC that was incubated for 5, 7.5 or 10 days. For BC incubated for 14 days, the culture medium was inoculated by directly adding 0.5 mL from bacteria stocks that were stored at -80 °C. BC incubated for 5 days was used for the filtration studies that compared DBC and NDBC. BC incubated for 5 or 10 days was used to investigate the effect of growth time on filtration performance. BC incubated for 10 days was used to evaluate the effect of POE addition to the culture medium as well as acetone treatment on the filtration performance. BC membranes grown for 5, 7.5 or 10 days were used for capillary flow porometry tests. A 14-day grown BC sample was used for filtration studies with BSA. After incubation, the formed BC pellicles were harvested and purified in 0.1 M NaOH at 60 °C for 4 h and washed thoroughly with DI water (never-dried BC,

NDBC). The purified pellicles were stored at 4 °C. To obtain dried BC (DBC), NDBC was dried between blotting papers and fabric on a 50 °C hot plate. Data on the density, thickness and porosity of the different types of BC used in this work is provided in Table S1 and the experimental details of these measurements are described in the Supplementary Information.

BC membranes incorporating POE (BC-POE) were produced by dissolving 10 g/L of POE (10 kDa) into the culture medium prior to adjusting pH, incubating for 10 days, and purifying the pellicles as described above. Acetone-treated BC membranes (BC-ac) were produced from BC incubated for 10 days without the addition of POE by solvent exchange with acetone after the purification step. A sheet of BC (≈ 8 cm x 14 cm) was immersed in acetone for 1 h and then the acetone was replaced 2 times. The membrane was left to dry in room temperature. BC grown for 14 days was used for TEMPO-oxidation (BC-TEMPO) after the purification step, following a previously reported method, where a charge density of ~250 μeq/g was reported (Orelma et al., 2014). Briefly, 0.1 g of TEMPO and 2.4 g of sodium bromide were dissolved in 500 mL of Milli-Q water and 13.4 mL of sodium hypochlorite solution (13 %) was added. The pH was adjusted to 10 with 1 M HCl. BC (≈ 10 cm x 15 cm) was immersed into the solution for 30 min and then in a 50 % ethanol solution to quench the reaction, followed by thorough washing with DI water.

2.3 Characterization

2.3.1 Scanning electron microscopy

The DBC samples that had been rewetted overnight in water were frozen at -80 °C and freeze-dried in a vacuum dryer (Labconco). Before imaging, the samples were sputter-coated with a 3 nm layer of platinum using a sputter coater (Leica). Samples were mounted on an aluminum stub using double sided carbon tape and imaged with a field emission scanning electron

microscope (Zeiss sigma VP, Carl Zeiss) using an acceleration voltage of 1.6 kV and working distance of 8 to 10 mm.

2.3.2 Capillary flow porometry

A capillary flow porometer (3gzh Quantachrome) was used for measurements of the bubble point of the samples. Details of the method are described in a previous study (Dumée et al., 2010). The DBC was wetted with water before measurement and the bubble points were determined using a pressure range of 1.4 to 20 bar for NDBC and from 3 to 32 bar for DBC.

2.4 Filtration experiments

DBC membranes were hydrated in DI water for a minimum of 12 h prior to conducting filtration experiments, to condition the membrane which swelled in water. Rehydrating the BC before experiments was observed to be critical in terms of flux. The schematics of the cross-flow unit and stirred cell are presented in Figure S1. It should be noted that the stirred cell provided the advantage of smaller processing volumes while the cross-flow set-up has the advantage of reducing concentration polarization.

2.4.1 Pure water flux and rejections of poly(oxyethylene) using cross-flow filtration

The cross-flow tests were carried out using a laboratory scale cross-flow unit (CF042, Sterlitech corporation) using Milli-Q water. The active membrane area was 42 cm^2. For flux hysteresis (recovery of flux when system pressure is decreased) experiments with NDBC and DBC membranes, the operating pressure was first increased every 30 min in steps (0.25, 0.5, 1, 1.5, 2 and 2.5 bar) and then was reduced every 30 min, also stepwise. The total duration of the experiment was 5.5 h. The flux was determined 30 min after each change of pressure. All other filtration tests, with the cross-flow unit, were conducted at a constant pressure of 2 bar and run for at least 1 h.

Prior to starting these tests, the membranes were compacted in the cross-flow unit at a pressure of 2.5 bar, for at least 30 min. After compaction, the PWF of the BC membranes at 2 bar was stable, as indicated by Figure S2. Each test was repeated at least three times using a new BC membrane for each run and results were calculated as an average of these runs. PWF (J) was determined using Equation (1)

$$J = \frac{V}{A\Delta t} \qquad (1),$$

where V is the volume of permeate (L), A is the active surface area of the membrane (m^2) and t is the permeation time (h). POE solutions were prepared in Milli-Q water at a concentration of 1 g/L. The tests for each POE of different molecular weight were continued for 1 h before collecting samples from the permeate and feed. During the 1 h operation, both the permeate and concentrate flows were returned to the feed. Tests were started with POE of the lowest molecular weight (0.1 MDa) and continued in order of increasing molecular weight without changing the BC membrane in between. The system and BC membrane were thoroughly cleaned with DI water before performing runs with POEs of different molecular weight. The cleaning was performed by running DI water through the system with the BC membrane still in place and then removing the membrane, rinsing it separately with DI water and running DI water through the unit, in the absence of the membrane. Samples from permeate and feed solutions were analyzed using a total organic carbon (TOC) analyzer (Shimadzu TOC-VCPH). The rejection of the POE was calculated using Equation (2)

$$R(\%) = \frac{C_f - C_p}{C_f} \times 100\% \qquad (2),$$

where C_f is the concentration of feed solution and C_p is the concentration of permeate.

2.4.2 Rejections of bovine serum albumin using stirred cell

BSA filtrations were performed with the unmodified, 14-days grown BC and TEMPO-oxidized BC. A stirred cell was used for BSA filtration experiments to allow smaller processing volumes. An Amicon 8200 stirred cell (Millipore) operated in dead-end mode, with an effective membrane area of 28.7 cm^2 and volume capacity of 200 mL was used. For the experiments, the cell was pressurized to 2 bar with compressed air. Filtration experiments were conducted for 60 min. A magnetic stirrer (RCT basic, IKA, stirring speed 2) was used for stirring. PWF and rejection were determined using equations (1) and (2).

BSA was dissolved in a phosphate buffered saline (PBS) solution (pH 7.4) and 50 mM sodium acetate buffers (pH 4, 5 and 6) to make solutions of 0.5 g/L. First, the stirred cell was filled with 100 mL of pH 7.4 solution. Permeate samples were collected at 30 min and 60 min after beginning each experiment. After 60 min filtration, the membrane was removed from the cell and washed thoroughly with deionized water. The washed membrane was placed back into the cell and the cell was filled with 100 mL pH 6 solution followed by solutions of pH 5 and pH 4. BSA concentration was determined from the permeate samples by measuring absorbance with a UV-Vis spectrophotometer (UV-2550, Shimadzu) at a wavelength of 280 nm. The filtration series for each type of membrane was repeated twice.

3 Results and discussion

3.1 Effect of drying and pressure on permeation properties of bacterial cellulose membranes

The pressure applied to BC membranes can influence their structure and therefore also their properties. Drying is another factor that significantly influences the properties of BC due to shrinkage and fiber aggregation. Herein the influence of these factors on the permeation properties of BC is addressed.

3.1.1 Effect of operating pressure on pure water flux and flux hysteresis of dried and never-dried bacterial cellulose membranes

First the influence of pressure on the flux of NDBC and DBC grown for 5 days was studied at operating pressures up to 2.5 bar, presenting a pressure range relevant for ultrafiltration and microfiltration. NDBC exhibits flux hysteresis (Figure 1), indicating compaction upon membrane compression as the pressure is increased. The thickness of NDBC membranes decreased 45% from their initial state when measured after the experiment (from 1.1±0.15 mm to 0.6±0.1 mm). In separate unconfined compression tests of NDBC, a compressive strain of 76% was measured under a compressive load of 2 bar (Figure S3). Inelastic behavior has been reported for BC under cyclic compression *in aqua* (Gao et al., 2015). This phenomenon is also suggested by the observations made here after use of NDBC in the cross-flow unit and from results of applying compressive load (note the sample "BC1" in Figure S3), indicating that after compression the BC network changed irreversibly.

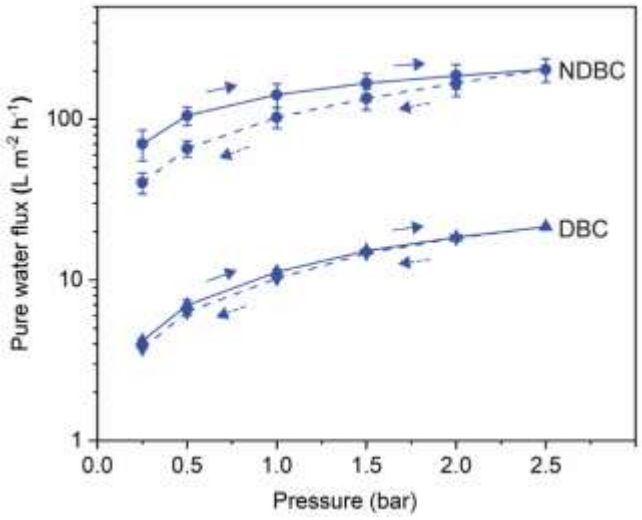

Figure 1 Effect of operating pressure on the pure water flux for never-dried (NDBC) and dried (DBC) membranes incubated for 5 days. Flux hysteresis, suggesting compaction of the BC network, was registered upon reducing the pressure, as indicated.

Compared to NDBC, the pure water flux (PWF) at 2.5 bar measured for the DBC membranes was 89% smaller (Figure 1), indicating drying-induced conformation changes in the BC matrix. Indeed, upon drying, the hydrated BC network collapses, leading to a reduced porosity that lowers the flux compared to NDBC. Considering the significantly higher thickness of the NDBC, the observed difference in water permeability is highlighted even further. Upon drying in air at 50 °C, the fiber network (BC grown for 5 days) was compressed by approximately 50-fold, from an initial thickness of 1100 µm to 23 µm. DBC has been reported to have a water retention (residual water content in the hydrogel after equilibration in water under its own weight) of 110%, remarkably lower than NDBC (water retention of 1030%) (Udhardt et al., 2005). While the PWF measured for DBC was significantly smaller than that for NDBC, the former displayed a relatively faster increase of PWF with pressure (going from 1 to 2 bar, a 39% flux increase was observed, compared with 24% in the case of NDBC). The more significant increase in PWF in the DBC

system compared to the NDBC can be explained by the densification of the NDBC structure due to the compaction caused by pressure increase. The DBC membrane showed limited hysteresis, indicating that no significant compression occurred during the experiment. Interestingly, for both DBC and NDBC, the proportional flux decreases at given pressure showed a decreasing trend from lower to higher pressure (Figure S4).

The values of PWF determined for the BC membranes (204 L m^{-2} h^{-1} and 21 L m^{-2} h^{-1} for NDBC and DBC at 2.5 bar, respectively) were in general lower than those reported for other membrane filtration materials; for instance, with cellulose acetate/polyethylene glycol ultrafiltration membranes (PWF of 360 L m^{-2} h^{-1} at 0.5 bar) (Mohammadi & Saljoughi, 2009) or with poly(vinyl chloride)/poly(carbonate) ultrafiltration membrane (PWF of 1260 L m^{-2} h^{-1} at 2 bar) (Behboudi et al., 2017). Nonetheless, it should be noted that the trade-off between flux and selectivity should be considered when discussing properties of separation membranes (Park et al., 2017). Therefore, membrane suitability should not be determined solely based on PWF values. When compared to typical commercial organic membranes, BC competes favorably as far as its sustainable production, without the use of hazardous chemicals or solvents, its high hydrophilicity (particularly in ND state), and resistance (to solvents, heat and chemicals). For nanopapers manufactured from BC, fluxes have been reported to depend on the grammage of the papers and the highest water permeance reported was 50 L m^{-2} $h^{-1}$$MPa^{-1}$ at a grammage of 10 g m^{-2} but decreased to < 10 L m^{-2} $h^{-1}$$MPa^{-1}$ for grammages > 40 g m^{-2} (Mautner et al., 2015).

The standard deviation of the measured PWF for NDBC was 23 to 130 times higher compared to the DBC system, at the corresponding pressure range. On the other hand, the fluxes were only 9 to 16 times higher in comparison. This suggests that the structure of NDBC was less homogeneous. The results emphasize the effect of both pressure and inelastic drying-induced

compression of BC membranes on their water permeability. These considerations are especially important for applications where fluid flux is critical.

3.1.2 Fluxes of never-dried and dried bacterial cellulose and rejections of poly(oxyethylene)s

The rejections of water-soluble POEs of varying average molecular weight, from 0.1 to 2 MDa, were evaluated using DBC and NDBC (Figure 2a). The upper limit of the hydrodynamic radius (R_h) for this POE series is estimated to be ~60 nm (2 MDa) (Devanand & Selser, 1991). For both NDBC and DBC membranes, the rejection significantly increased as the POE R_h was increased e.g., going from a molecular weight of 0.1 MDa until reaching a plateau for POE 0.4 MDa ($R_h \approx 20$ nm) for the NDBC membrane. The same was observed for the DBC membranes except that the plateau was reached at larger POE molecular sizes (1 MDa, equivalent to $R_h \approx 40$ nm). In the case of DBC, the increase in rejection (from 71% to 81%) going form POE of 0.4 MDa to 1 MDa, was much lower than the increase in rejection observed with NDBC (from 7% to 71%). For the NDBC membranes, POE rejection of 2 MDa (54%) was slightly lower than for the 1 MDa sample (61%), which is likely the result of experimental artifacts, possibly caused by variation in permeate concentrations over time and the presence of larger defects across the planar areas of BC. As expected, based on the PWF results and flux-selectivity tradeoff typically exhibited by membranes (Park et al., 2017), the rejections were higher with DBC compared to NDBC, with the highest rejection (82%) noted for POE of 2 MDa, slightly higher than for POE of 1 MDa (81%). However, the rejections achieved here with 0.1 MDa POE (6% and 7% with DBC and NDBC, respectively) were very low when compared with rejection reported for nanopapers manufactured from BC (75% rejection for 93 kDa POE) (Mautner et al., 2015).

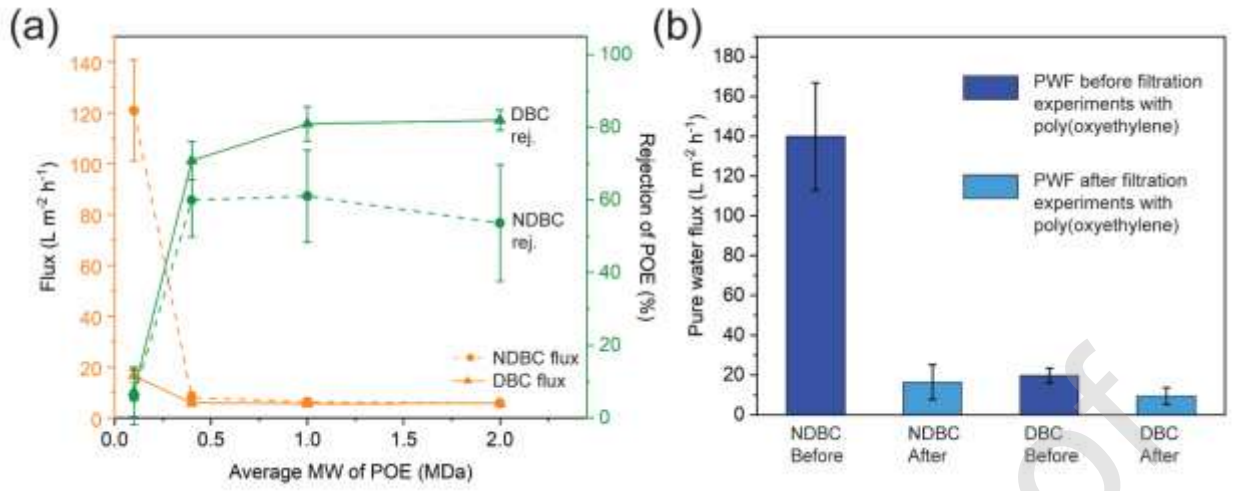

Figure 2 Filtration of POE solutions with varying average molecular weight using BC membranes: (a) Dependence of rejection and flux on POE molecular weight for never-dried (NDBC) and dried (DBC) membranes. (b) Pure water fluxes of BC at 2 bar before starting filtration experiments with POEs and after consecutive filtration experiments with POEs of average molecular weights 0.1 MDa, 0.4 MDa, 1 MDa and 2 MDa.

A significant decrease in POE solution flux (going from 0.1 MDa to 0.4 MDa) was observed for both NDBC and DBC: 93% and 65%, respectively. This observation suggests that for both membranes, significant adsorption and pore clogging occurred with the larger POE size (0.4 MDa). POE is known to adsorb onto silica (Flood et al., 2006; Mathur & Moudgil, 1997), resulting in a hydrodynamic layer thickness of approximately 5 nm for a POE molecular weight of 0.1 MDa (and approximately 30 nm for 1 MDa POE) (Pattanayek & Juvekar, 2002). The adsorption of POE on cellulose nanocrystals has also been studied and POE of molecular weight 0.6 MDa has been shown to adsorb on the nanocrystals (Oguzlu & Boluk, 2017). Therefore, it is likely that POE adsorption occurred on BC, resulting in a reduction of the effective average pore

size and a substantial decrease in flux shortly after initiating the filtration with 0.4 MDa POE. This is further supported by evaluating the PWF before and after using BC membranes in cross-flow experiments with the series of POEs having different molecular sizes: a PWF reduction of 86% and 42% was observed for NDBC and DBC, respectively (Figure 2b). Since, the relative reduction was clearly more extensive for the NDBC, these results suggest that the structure of the NDBC was more significantly affected by the adsorption of POE. The rejection and flux results, particularly after the experiment with the 0.4 MDa POE, are likely influenced by POE adsorbed onto the membranes. However, when the molecular weight of POE increases, larger POE chains may replace previously adsorbed smaller POEs. For instance, such effects have been reported on silica surfaces (Fu & Santore, 1998; Rebar & Santore, 1996). The fluxes reported in Figure 2a also indicate that for both DBC and NDBC, no significant reduction in flux is observed in experiments conducted with 1 MDa and 2 MDa POE. Based on these results and the fact that the BC network structure is inhomogeneous across the principal plane, it is likely that most of the pores in the network were affected by adsorption of the 0.4 MDa POE, but a small amount of significantly larger pores, that were not clogged, were also present in the network.

While the pore size of BC has been assessed by using nitrogen sorption, SEM, mercury intrusion porometry and thermoporometry (Pircher et al., 2014), many of the techniques used have significant limitations in terms of the pore size range that can be reliably analyzed. This poses a challenge when considering the broad pore size distributions of BC membranes. Pore size analysis typically requires for the sample to be dry. Attempts to analyze the pore sizes of native cellulose, such as NDBC, involve the confounding effect that drying has on the structure; therefore, critical point drying with carbon dioxide has been used to limit such effects (e.g., shrinkage of the BC network). Such drying and subsequent use of nitrogen sorption, thermoporometry and SEM

analyses have indicated that BC has a wide distribution of pore sizes, from the nano to the micrometer range (Pircher et al., 2014). For DBC, mean pore diameters of 23 and 28 nm were determined by thermoporometry and nitrogen sorption, respectively (Kaewnopparat et al., 2008). Based on the results related to POE rejection in our experiments with NDBC and DBC, the challenges related to typical pore characterization techniques and the impact of pressure on the membrane network, it can be concluded that values reported in literature for pore sizes of BC cannot be directly used to evaluate the molecular size of the molecules that are rejected by the membranes. The results on the filtration properties of BC from this work provide indirect insights on the pore structure of BC when in aqueous conditions and subjected to pressure, which would not be attainable with the traditional pore characterization methods introduced above.

3.1.3 Pressure response and associated dewatering of wet never-dried and dried bacterial cellulose membranes obtained from varying incubation time

Due to the importance of network topology for filtration performance, and more importantly, the applied operating pressure, the mechanical response and associated fluid flow using NDBC and DBC was evaluated (Figure 3). More specifically, pre-wetted BC membranes obtained after given incubation times, namely, 5, 7.5 and 10 days, were studied. For this purpose, a special capillary flow porometry setup was used. We note that capillary flow porometry is not reliable to determine the pore sizes of the BC network, due to compression that occurs during the measurement. Nevertheless, the results are indicative of the relative behavior of the DBC and NDBC membranes, which were obtained after different incubation times. The pressure at the onset of flow through, or bubble point (BP), showed that compression of the membranes, associated with water loss and flow through, occurred at a low pressure for the NDBC membranes. In contrast, a significantly higher pressure was required for the DBC membrane. A clear trend of increasing BP

was observed as a function of the BC incubation time for both DBC and NDBC, suggesting that changes in the network structure and reduced pore size occurred as the incubation time used to obtain the membrane was increased. A longer incubation leads to a denser BC structure, resulting in a stronger BC network (W. Tang et al., 2010; Yao et al., 2013).

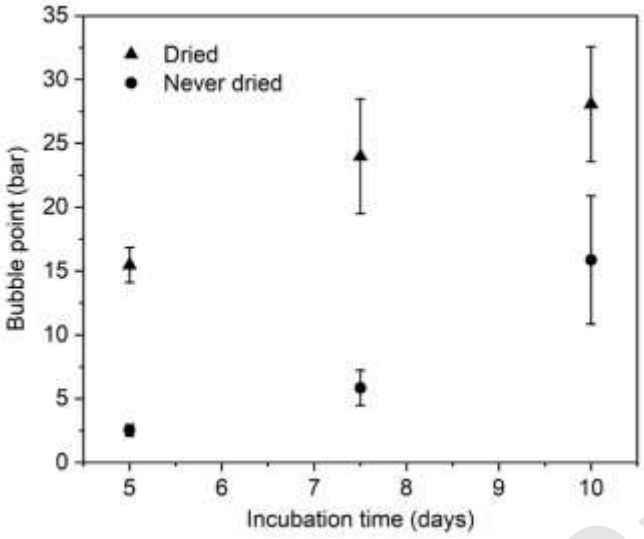

Figure 3 Bubble points for NDBC and DBC membranes measured by capillary flow porometry. The bubble point refers to the onset of flow through in the measurement.

3.2 Impact of incubation time and modification on the permeation properties of dried bacterial cellulose membranes

Next the surface morphology and the filtration properties of acetone-treated BC membranes (BC-ac), BC membranes incorporating POE (BC-POE) and unmodified BC produced after 5- and 10-days incubation time was evaluated.

3.2.1 Pure water fluxes and rejections of poly(oxyethylene)s for modified and unmodified bacterial cellulose membranes

The addition of 4 kDa POE to the culture medium has been reported to decrease the pore sizes in the BC network, whereas addition of 0.4 kDa POE was reported to increase pore sizes based on observations from SEM images (Heßler & Klemm, 2009). Addition of 0.1 MDa POE to the culture medium at various concentrations has also been studied and increasing the concentration of POE was reported to cause larger bundles of aggregated BC nanofibers in the network (Brown & Laborie, 2007). Increasing the porosity of nanocellulose films with organic solvents, such as acetone, has been demonstrated (Henriksson et al., 2008; Karim et al., 2016). Therefore, the effects of acetone treatment and 10 kDa POE addition to the culture medium on the filtration performance of BC were investigated.

SEM images of the BC membranes indicate that BC-ac had a more porous and open structure compared to BC-POE and unmodified BC (Figure 4a-d). Meanwhile, BC-POE displayed a slightly denser network compared to unmodified BC (see low magnification images in Figure S5). The SEM images provided comparative insights on the networks but since drying causes structural changes in BC, SEM does not reflect the structure of the nanofibrous network in the wet state (Clasen et al., 2006). Thus, to some degree, more insightful information can be gained by comparing the filtration properties (Figure 4e).

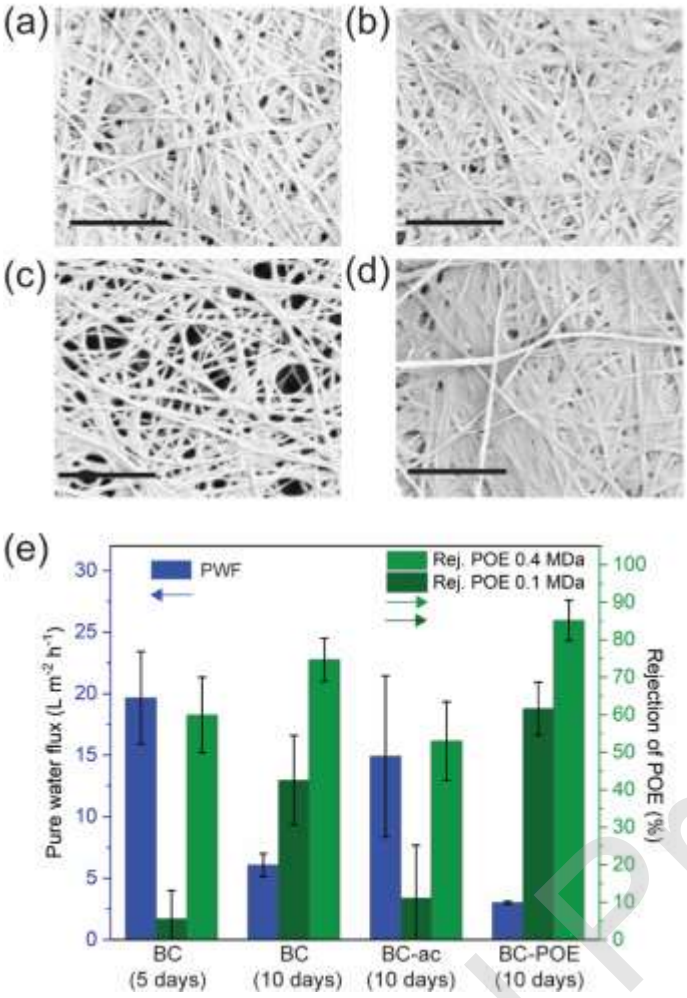

Figure 4 SEM images of (a) BC membranes obtained after incubation for 5 and (b) 10 days. (c) Acetone-treated BC membrane obtained after incubation for 10 days (d) membranes obtained by incubation for 10 days in the presence of poly(oxyethylene) (POE) in the culture medium. Scale bars are 1 µm. (e) Effect of incubation time, acetone treatment (BC-ac) and addition of POE to culture medium (BC-POE) on pure water flux and POE rejection of dried BC.

As expected, the PWF decreases for BC membranes produced after longer incubation times. A 69% PWF reduction was measured going from membranes obtained during short (5 days) to the

longer (10 days) incubation time. When normalizing the PWF using the membrane thickness, the corresponding reduction is 75%. These results, along with the discussion in 3.1.3, suggest that in addition to an increased membrane thickness, a higher degree of (physical) interfibrillar cross-links existed in BC sheets grown during a longer incubation time. The POE rejection showed a significant increase when the incubation time used to produce the BC membranes was doubled, from 5 to 10 days, especially if looking at the 0.1 MDa POE rejection, where an increase of 87% was observed. The thickness, density and porosity data (Table S1), indicate that when the incubation time increased from 5 to 10 days, the thickness and density increased by 30% and 49%, respectively, and the porosity decreased by 18%.

Due to the higher rejections achieved with BC obtained after incubation for 10 days, this membrane was used to further study the impact of membrane pre-treatment. Compared to unmodified BC, acetone treatment followed by drying and rehydration resulted in a significantly higher flux (increase of 145%). This is potentially the result of smaller capillary stresses during drying leading to a reduced nanofiber network collapse. An even more significant increase in PWF due to acetone treatment (from 4 to 25 L m^{-2} h^{-1}) has been reported for cellulose nanofibril membranes (Karim et al., 2016). In contrast, growing the BC pellicles in the presence of POE resulted in a significant flux reduction (51 %), suggesting an overall more densified network, as also indicated by SEM imaging. Interestingly, an increase in surface roughness was also observed for the BC-POE membrane compared to the unmodified reference (Figure S6), which likely influences the observed permeation properties. As expected, the trend in flux values corresponded well with the rejections determined for POE of average molecular weight 0.1 MDa and 0.4 MDa when comparing to unmodified BC, with higher rejections in the case of BC-POE and lower rejections in the case of BC-ac. It should be noted that when comparing the results of BC-ac

incubated for 10 days and BC incubated for 5 days, the PWF results do not correlate with SEM observations. Compared to BC incubated for 5 days, the SEM images clearly indicate a more porous surface structure in the BC-ac sample; however, the flux of BC-ac was lower compared to BC incubated for 5 days. In contrast with what the SEM analysis would infer, the trend in the density data shown in Table S1 correlates with the PWF results since the densities of the samples were in the order of BC-POE (10 days) > BC (10 days) > BC-ac (10 days) > BC (5 days). It should also be noted that the standard deviation in the PWF results of the BC-ac sample was large.

3.2.2 The effect of surface charge on protein rejection of bacterial cellulose membranes

The PWF of BC membranes produced after incubation for 14 days was investigated using cross-flow and dead-end (stirred cell) units. A PWF of 5.3 L m^{-2} h^{-1} was measured with the cross-flow unit compared to a flux of 10.5 L m^{-2} h^{-1} determined with the stirred cell, at a pressure of 2 bar. This further emphasizes the effect of the pressure gradient, which is more prominent in a dead-end, stirred cell, compared with the homogeneous pressure across the surface of the BC membranes in the case of the cross-flow unit. The following discussion refers to results obtained with a dead-end stirred cell.

Treatment of BC membranes by addition of secondary components such as particles or macromolecules, or by chemical modification, such as oxidation, has been reported for given purposes (Heßler & Klemm, 2009; Orelma et al., 2014). Herein BC membranes were modified by TEMPO-oxidation, introducing negative charges on the membrane at pH above 4, due to dissociation of carboxyl groups. TEMPO-oxidation of the BC membranes clearly decreased the PWF, since a decrease of 54 % was observed compared to unmodified BC (Figure S7).

In order to further assess the effect of membrane charge, the rejection of a model protein (BSA) was evaluated. BSA has a point of neutral charge at pH 4.7 (the isoelectric point, IEP), above which it becomes negatively charged (while below this pH a net positive charge is present). Based on zeta potential measurements, the electrostatic charges of TEMPO-oxidized BC were significantly higher (from -33 to -42 mV) compared to unmodified BC (from -4 to -8 mV) in the pH range used for the BSA separation experiments (Figure S8). The BC surface charge greatly influenced the rejection of BSA (Figure 5). In the case of unmodified BC, there was no significant effect of pH on BSA rejection (only a slight reduction in rejection was observed as BSA became more negatively charged at high pH). In sharp contrast, for the TEMPO-modified BC, the absence of negative charges on the protein resulted in a near complete rejection of albumin, which sharply decreased upon increasing the pH above its IEP. The membrane was negatively charged at pH 4 and 5 and the high rejection is likely the result of the formation of BSA aggregates on the oppositely charged membrane, particularly at pH 4.

The impact of pH on BSA separation has been studied for other membrane systems, including chitosan/polystyrene sulfonate multilayer membranes (Aravind et al., 2007), quaternized polysulfone including graphene oxide nanosheets (Kumar et al., 2015), ceramic membranes (de la Casa et al., 2007), and negatively charged inorganic-organic hybrid membranes (Kumar & Lawler, 2014). These studies demonstrated that the pH of the solution and the membrane charge significantly influence BSA rejection, as observed also in this work. In these studies, the maximum rejection reported for BSA ranged from 95% to 100%. These studies also reported similar effects on the rejection of BSA when the membrane and BSA were oppositely charged, as was observed here for the TEMPO-oxidized BC. This has been explained by the formation of a self-rejecting layer of BSA on the membrane surface (Kumar et al., 2015). The quaternized polysulfone graphene

oxide nanosheet membrane showed increased BSA rejection at pH 7 and 11, when BSA and the membrane were oppositely charged. (Kumar et al., 2015). For inorganic-organic hybrid membranes, a high BSA rejection at pH 3 was achieved. However, even higher rejections were observed at pH 11 when the membrane and BSA were both negatively charged (Kumar & Lawler, 2014).

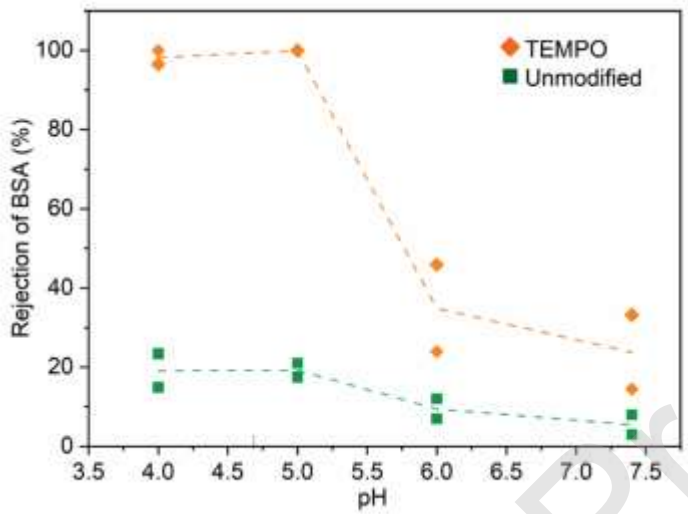

Figure 5 Rejection of BSA by TEMPO-oxidized and unmodified BC. The points indicate the results from individual experiments and the dashed lines are drawn to indicate the trend in rejection values.

2D and 3D BC materials are attractive for biomedical applications (Greca et al., 2018; Zang et al., 2015), where a range of complex fluids may permeate through the nanofiber network at varying pressures. The range of macromolecules and BC networks evaluated in the previous sections highlight the fact that based on size exclusion principles, BC membranes are permeable to most proteins, while the permeability decreases upon fouling. However, our results indicate that separation based on molecular affinity is also possible by judiciously introducing surface charges on BC, based on the isoelectric point (IEP) of target proteins and filtering solution pH. Therefore,

when considering complex fluids permeability across BC, it will be quintessential to consider the species to be permeated in order to determine the optimal BC membrane modification or pre-treatment.

4 Conclusions and prospects

The main findings of this study are summarized as follow: (1) Cross-flow experiments and capillary flow porometry showed that NDBC and DBC perform quite differently under pressure, with NDBC showing significant compression. (2) Differences in DBC and NDBC significantly affect the flux and rejection values measured for POEs, with NDBC having significantly higher PWF and consequently lower rejection. (3) The effects of incubation time and treatment are demonstrated with DBC, indicating the possibility of adjusting the PWF. (4) Separation with unmodified BC membranes is challenging due to the low macromolecular rejections but, in the case of charged solutes, the BC surface charge can be conveniently modified to enable separation.

The filtration properties of BC are strongly related to the BC network structure, which depends on the incubation conditions and post-culture treatments used. For future studies on permeation properties of BC, particles of well-defined size may be useful for defining the molecular weight cut-off of DBC and NDBC. In terms of size-exclusion, removal of viruses from aqueous environments could be investigated. As more intricate understanding of biofabrication is developing in parallel to the exploration of BC in the biomedical field, the insights of this study can be useful in determining the long-term response of such materials *in-vivo*. Other endeavors for filtration using BC membranes may also be considered, particularly where a high turnover rate of membranes would warrant a “green”-sourced membrane.

CRediT authorship contribution statement

Janika Lehtonen: Conceptualization, Methodology, Investigation, Writing – Original Draft, Visualization **Xiao Chen:** Investigation, Writing – Review & editing **Marco Beaumont:** Investigation, Writing – Review & editing **Jukka Hassinen:** Conceptualization, Writing – Review & editing **Hannes Orelma:** Conceptualization, Writing – Review & editing **Ludovic F. Dumée:** Conceptualization, Writing – Review & editing, Supervision **Blaise L. Tardy:** Conceptualization, Writing – Original draft, Supervision **Orlando J. Rojas:** Conceptualization, Writing – Review & editing, Supervision, Funding

Declarations of competing interest

The authors declare no competing interest.

Acknowledgement

This work was funded by H2020-ERC-2017-Advanced Grant "BioELCell" (788489). This work was a part of the Academy of Finland's Flagship Programme under Projects No. 318890 and 318891 (Competence Center for Materials Bioeconomy, FinnCERES). LD acknowledges the Australian Research Council (ARC) for his Discovery Early Career Researcher Award (DECRA) 2018 (180100130). OJR is also grateful to the Canada Excellence Research Chair initiative. We acknowledge the facilities and technical support by Aalto University OtaNano Nanomicroscopy center (Aalto-NMC).

References

Abedini, R., Mousavi, S. M., & Aminzadeh, R. (2011). A novel cellulose acetate (CA) membrane

using TiO2 nanoparticles: Preparation, characterization and permeation study. *Desalination*, *277*(1–3), 40–45. https://doi.org/10.1016/j.desal.2011.03.089

Aravind, U. K., Mathew, J., & Aravindakumar, C. T. (2007). Transport studies of BSA, lysozyme and ovalbumin through chitosan/polystyrene sulfonate multilayer membrane. *Journal of Membrane Science*, *299*(1–2), 146–155. https://doi.org/10.1016/j.memsci.2007.04.036

Behboudi, A., Jafarzadeh, Y., & Yegani, R. (2017). Polyvinyl chloride/polycarbonate blend ultrafiltration membranes for water treatment. *Journal of Membrane Science*, *534*, 18–24. https://doi.org/10.1016/j.memsci.2017.04.011

Brown, E. E., & Laborie, M. P. G. (2007). Bioengineering bacterial cellulose/poly(ethylene oxide) nanocomposites. *Biomacromolecules*, *8*(10), 3074–3081. https://doi.org/10.1021/bm700448x

Camacho, L. M., Dumée, L., Zhang, J., Li, J. de, Duke, M., Gomez, J., & Gray, S. (2013). Advances in membrane distillation for water desalination and purification applications. *Water (Switzerland)*, *5*(1), 94–196. https://doi.org/10.3390/w5010094

Carreño Pineda, L. D., Caicedo Mesa, L. A., & Habert, A. C. (2010). Effect of culture and purification conditions on physicochemical and transport properties in bacterial cellulose membranes. *Chemical Engineering Transactions*, *20*, 327–330. https://doi.org/10.3303/CET1020055

Clasen, C., Sultanova, B., Wilhelms, T., Heisig, P., & Kulicke, W. (2006). Effects of Different Drying Processes on the Material Properties of Bacterial Cellulose Membranes. *Macromolecular Symposia*, *244*, 48–58. https://doi.org/10.1002/masy.200651204

de la Casa, E. J., Guadix, A., Ibáñez, R., & Guadix, E. M. (2007). Influence of pH and salt concentration on the cross-flow microfiltration of BSA through a ceramic membrane. *Biochemical Engineering Journal*, *33*(2), 110–115. https://doi.org/10.1016/j.bej.2006.09.009

Devanand, K., & Selser, J. C. (1991). Asymptotic Behavior and Long-Range Interactions in Aqueous Solutions of Polyethylene oxide. *Macromolecules*, *24*, 5943–5947. https://doi.org/10.1021/ma00022a008

Dubey, V., Saxena, C., Singh, L., Ramana, K. V., & Chauhan, R. S. (2002). Pervaporation of binary water-ethanol mixtures through bacterial cellulose membrane. *Separation and Purification Technology*, *27*(2), 163–171. https://doi.org/10.1016/S1383-5866(01)00210-6

Dumée, L., Sears, K., Schütz, J., Finn, N., Duke, M., & Gray, S. (2010). A preliminary study on the effect of macro cavities formation on properties of carbon nanotube bucky-paper composites. *Materials*, *4*(3), 553–561. https://doi.org/10.3390/ma4030553

Flood, C., Cosgrove, T., Howell, I., & Revell, P. (2006). Effects of electrolytes on adsorbed polymer layers: Poly(ethylene oxide)-silica system. *Langmuir*, *22*(16), 6923–6930. https://doi.org/10.1021/la060724+

Fu, L., Zhou, P., Zhang, S., & Yang, G. (2013). Evaluation of bacterial nanocellulose-based uniform wound dressing for large area skin transplantation. *Materials Science & Engineering C*, *33*(5), 2995–3000. https://doi.org/10.1016/j.msec.2013.03.026

Fu, Z., & Santore, M. M. (1998). Kinetics of competitive adsorption of PEO chains with different molecular weights. *Macromolecules*, *31*(20), 7014–7022. https://doi.org/10.1021/ma980042w

Galdino, C. J. S., Maia, A. D., Meira, H. M., Souza, T. C., Amorim, J. D. P., Almeida, F. C. G., Costa, A. F. S., & Sarubbo, L. A. (2020). Use of a bacterial cellulose filter for the removal of oil from wastewater. *Process Biochemistry*, *91*, 288–296. https://doi.org/10.1016/j.procbio.2019.12.020

Gao, X., Shi, Z., Liu, C., Yang, G., Sevostianov, I., & Silberschmidt, V. V. (2015). Inelastic behaviour of bacterial cellulose hydrogel : In aqua cyclic tests. *Polymer Testing*, *44*, 82–92. https://doi.org/10.1016/j.polymertesting.2015.03.021

Gelin, K., Bodin, A., Gatenholm, P., Mihranyan, A., Edwards, K., & Strømme, M. (2007). Characterization of water in bacterial cellulose using dielectric spectroscopy and electron microscopy. *Polymer*, *48*(26), 7623–7631. https://doi.org/10.1016/j.polymer.2007.10.039

George, J., Sajeevkumar, V. A., Kumar, R., Ramana, K. V, Sabapathy, S. N., & Bawa, A. S. (2008). Enhancement of thermal stability associated with the chemical treatment of bacterial (Gluconacetobacter xylinus) cellulose. *Journal of Applied Polymer Science*, *108*(3), 1845–1851. https://doi.org/10.1002/app.27802

Gonçalves, S., Padrão, J., Rodrigues, I. P., Silva, J. P., Sencadas, V., Lanceros-Mendez, S., Girão, H., Dourado, F. & Rodrigues, L. R. (2015). Bacterial Cellulose As a Support for the Growth of Retinal Pigment Epithelium. *Biomacromolecules*, *16*(4), 1341-1351. https://doi.org/10.1021/acs.biomac.5b00129

Greca, L. G., Lehtonen, J., Tardy, B. L., Guo, J., & Rojas, O. J. (2018). Biofabrication of multifunctional nanocellulosic 3D structures: A facile and customizable route. *Materials Horizons*, *5*(3), 408–415. https://doi.org/10.1039/c7mh01139c

Hassan, E., Hassan, M., Abou-zeid, R., & Berglund, L. (2017). Use of Bacterial Cellulose and Crosslinked Cellulose Nanofibers Membranes for Removal of Oil from Oil-in-Water Emulsions. *Polymers*, *9*(9), 1-14. https://doi.org/10.3390/polym9090388

Henriksson, M., Berglund, L. A., Isaksson, P., Lindström, T., & Nishino, T. (2008). Cellulose nanopaper structures of high toughness. *Biomacromolecules*, *9*(6), 1579–1585. https://doi.org/10.1021/bm800038n

Heßler, N., & Klemm, D. (2009). Alteration of bacterial nanocellulose structure by in situ modification using polyethylene glycol and carbohydrate additives. *Cellulose*, *16*(5), 899–910. https://doi.org/10.1007/s10570-009-9301-5

Jiang, Q., Ghim, D., Cao, S., Tadepalli, S., Liu, K. K., Kwon, H., Luan, J., Min, Y., Jun, Y. S., & Singamaneni, S. (2019). Photothermally Active Reduced Graphene Oxide/Bacterial Nanocellulose Composites as Biofouling-Resistant Ultrafiltration Membranes. *Environmental Science and Technology*, *53*(1), 412–421. https://doi.org/10.1021/acs.est.8b02772

Iguchi, M., Yamanaka, S., & Budhiono (2000). Bacterial cellulose — a masterpiece of nature ' s arts. *Journal of Materials Science*, 35, 261–270.

Kaewnopparat, S., Sansernluk, K., & Faroongsarng, D. (2008). Behavior of freezable bound water in the bacterial cellulose produced by Acetobacter xylinum: An approach using thermoporosimetry. *AAPS PharmSciTech*, *9*(2), 701–707. https://doi.org/10.1208/s12249-008-9104-2

Karim, Z., Claudpierre, S., Grahn, M., Oksman, K., & Mathew, A. P. (2016). Nanocellulose based functional membranes for water cleaning : Tailoring of mechanical properties , porosity and

metal ion capture. *Journal of Membrane Science*, *514*, 418–428. https://doi.org/10.1016/j.memsci.2016.05.018

Klemm, D., Kramer, F., Moritz, S., Lindström, T., Ankerfors, M., Gray, D., & Dorris, A. (2011). Nanocelluloses : A New Family of Nature-Based Materials. *Angewandte*, *50*(24), 5438–5466. https://doi.org/10.1002/anie.201001273

Kumar, M., & Lawler, J. (2014). Preparation and characterization of negatively charged organic-inorganic hybrid ultrafiltration membranes for protein separation. *Separation and Purification Technology*, *130*, 112–123. https://doi.org/10.1016/j.seppur.2014.04.027

Kumar, M., McGlade, D., Ulbricht, M., & Lawler, J. (2015). Quaternized polysulfone and graphene oxide nanosheet derived low fouling novel positively charged hybrid ultrafiltration membranes for protein separation. *RSC Advances*, *5*(63), 51208–51219. https://doi.org/10.1039/c5ra06893b

Leitch, M. E., Li, C., Ikkala, O., Mauter, M. S., & Lowry, G. V. (2016). Bacterial Nanocellulose Aerogel Membranes: Novel High-Porosity Materials for Membrane Distillation. *Environmental Science and Technology Letters*, *3*(3), 85–91. https://doi.org/10.1021/acs.estlett.6b00030

Liebert, T. (2010). Cellulose Solvents - Remarkable History, Bright Future. In *Cellulose Solvents: For Analysis, Shaping and Chemical Modification* (pp. 3–54). https://doi.org/10.1021/bk-2010-1033.ch001

Mathur, S., & Moudgil, B. M. (1997). Adsorption Mechanism(s) of Poly(Ethylene Oxide) on Oxide Surfaces. *Journal of Colloid and Interface Science*, *98*(196), 92–98.

Mautner, A., Lee, K. Y., Tammelin, T., Mathew, A. P., Nedoma, A. J., Li, K., & Bismarck, A. (2015). Cellulose nanopapers as tight aqueous ultra-filtration membranes. *Reactive and Functional Polymers*, *86*, 209–214. https://doi.org/10.1016/j.reactfunctpolym.2014.09.014

Mohammadi, T., & Saljoughi, E. (2009). Effect of production conditions on morphology and permeability of asymmetric cellulose acetate membranes. *Desalination*, *243*(1–3), 1–7. https://doi.org/10.1016/j.desal.2008.04.010

Nishi, Y., Uryu, M., Yamanaka, S., Watanabe, K., Kitamura, N., Iguchi, M., & Mitsuhashi, S. (1990). The structure and mechanical properties of sheets prepared from bacterial cellulose - Part 2 Improvement of the mechanical properties of sheets and their applicability to diaphragms of electroacoustic transducers. *Journal of Materials Science*, *25*(6), 2997–3001. https://doi.org/10.1007/BF00584917

Oguzlu, H., & Boluk, Y. (2017). Interactions between cellulose nanocrystals and anionic and neutral polymers in aqueous solutions. *Cellulose*, *24*(1), 131–146. https://doi.org/10.1007/s10570-016-1096-6

Orelma, H., Morales, L. O., Johansson, L. S., Hoeger, I. C., Filpponen, I., Castro, C., Rojas, O. J., & Laine, J. (2014). Affibody conjugation onto bacterial cellulose tubes and bioseparation of human serum albumin. *RSC Advances*, *4*(93), 51440–51450. https://doi.org/10.1039/c4ra08882d

Pandey, L. K., Saxena, C., & Dubey, V. (2005). Studies on pervaporative characteristics of bacterial cellulose membrane. *Separation and Purification Technology*, *42*(3), 213–218. https://doi.org/10.1016/j.seppur.2004.07.014

Park, H. B., Kamcev, J., Robeson, L. M., Elimelech, M., & Freeman, B. D. (2017). Maximizing

the right stuff: The trade-off between membrane permeability and selectivity. *Science*, *356*(6343), 1138–1148. https://doi.org/10.1126/science.aab0530

Pattanayek, S. K., & Juvekar, V. A. (2002). Prediction of adsorption of nonionic polymers from aqueous solutions to solid surfaces. *Macromolecules*, *35*(25), 9574–9585. https://doi.org/10.1021/ma020478i

Pircher, N., Veigel, S., Aigner, N., Nedelec, J. M., Rosenau, T., & Liebner, F. (2014). Reinforcement of bacterial cellulose aerogels with biocompatible polymers. *Carbohydrate Polymers*, *111*, 505–513. https://doi.org/10.1016/j.carbpol.2014.04.029

Plappert, S. F., Nedelec, J. M., Rennhofer, H., Lichtenegger, H. C., & Liebner, F. W. (2017). Strain Hardening and Pore Size Harmonization by Uniaxial Densification: A Facile Approach toward Superinsulating Aerogels from Nematic Nanofibrillated 2,3-Dicarboxyl Cellulose. *Chemistry of Materials*, *29*(16), 6630–6641. https://doi.org/10.1021/acs.chemmater.7b00787

Rebar, V. A., & Santore, M. M. (1996). Molecular weight effects and the sequential dynamic nature of poly(ethylene oxide) adsorption on silica from polydisperse aqueous solution. *Macromolecules*, *29*(19), 6273–6283. https://doi.org/10.1021/ma951237w

Roig-Sanchez, S., Jungstedt, E., Anton-Sales, I., Malaspina, D. C., Faraudo, J., Berglund, L. A., Laromaine, A., & Roig, A. (2019). Nanocellulose films with multiple functional nanoparticles in confined spatial distribution. *Nanoscale Horizons*, *4*(3), 634–641. https://doi.org/10.1039/c8nh00310f

Shibazaki, H., Kuga, S., Onabe, F., & Usuda, M. (1993). Bacterial cellulose membrane as separation medium. *Journal of Applied Polymer Science*, *50*, 965–969.

Sokolnicki, A. M., Fisher, R. J., Harrah, T. P., & Kaplan, D. L. (2006). Permeability of bacterial cellulose membranes. *Journal of Membrane Science*, *272*, 15–27. https://doi.org/10.1016/j.memsci.2005.06.065

Tabuchi, M., & Baba, Y. (2005). Design for DNA separation medium using bacterial cellulose fibrils. *Analytical Chemistry*, *77*(21), 7090–7093. https://doi.org/10.1021/ac0511389

Takai, M., Nonomura, F., Inukai, T., Fujiwara, M., & Hayashi, J. (1991). Filtration and permeation characteristics of bacterial cellulose composite. *Sen'i Gakkaishi*, *47*(3), 119–129. https://doi.org/10.2115/fiber.47.119

Tang, N., Zhang, S., Si, Y., Yu, J., & Ding, B. (2019). An ultrathin bacterial cellulose membrane with a Voronoi-net structure for low pressure and high flux microfiltration. *Nanoscale*, *11*(38), 17851–17859. https://doi.org/10.1039/c9nr06028f

Tang, W., Jia, Æ. S., & Jia, Æ. Y. (2010). The influence of fermentation conditions and post-treatment methods on porosity of bacterial cellulose membrane. *World Journal of Microbiology and Biotechnology*, *26*, 125–131. https://doi.org/10.1007/s11274-009-0151-y

Tripathi, A., Tardy, B. L., Khan, S. A., Liebner, F., & Rojas, O. J. (2019). Expanding the upper limits of robustness of cellulose nanocrystal aerogels: Outstanding mechanical performance and associated pore compression response of chiral-nematic architectures. *Journal of Materials Chemistry A*, *7*(25), 15309–15319. https://doi.org/10.1039/c9ta03950c

Udhardt, U., Hesse, S., & Klemm, D. (2005). Analytical investigations of bacterial cellulose. *Macromolecular Symposia*, *223*, 201–212. https://doi.org/10.1002/masy.200550514

Ul-islam, M., Khan, T., & Kon, J. (2012). Water holding and release properties of bacterial

cellulose obtained by in situ and ex situ modification. *Carbohydrate Polymers*, *88*(2), 596–603. https://doi.org/10.1016/j.carbpol.2012.01.006

Wu, Z. Y., Li, C., Liang, H. W., Chen, J. F., & Yu, S. H. (2013). Ultralight, flexible, and fire-resistant carbon nanofiber aerogels from bacterial cellulose. *Angewandte Chemie - International Edition*, *52*(10), 2925–2929. https://doi.org/10.1002/anie.201209676

Xu, T., Jiang, Q., Ghim, D., Liu, K. K., Sun, H., Derami, H. G., Wang, Z., Tadepalli, S., Jun, Y. S., Zhang, Q., & Singamaneni, S. (2018). Catalytically Active Bacterial Nanocellulose-Based Ultrafiltration Membrane. *Small*, *14*(15), 1–8. https://doi.org/10.1002/smll.201704006

Yao, W., Wu, X., Zhu, J., Sun, B., & Miller, C. (2013). In vitro enzymatic conversion of γ-aminobutyric acid immobilization of glutamate decarboxylase with bacterial cellulose membrane (BCM) and non-linear model establishment. *Enzyme and Microbial Technology*, *52*(4–5), 258–264. https://doi.org/10.1016/j.enzmictec.2013.01.008

Zang, S., Zhang, R., Chen, H., Lu, Y., Zhou, J., Chang, X., Qiu, G., Wu, Z., & Yang, G. (2015). Investigation on artificial blood vessels prepared from bacterial cellulose. *Materials Science and Engineering C*, *46*, 111–117. https://doi.org/10.1016/j.msec.2014.10.023